System identification for the control of wind turbine systems

Ivo Houtzager
I.Houtzager@TUDelft.nl

Balázs Kulcsár
B.A.Kulcsar@TUDelft.nl

Jan-Willem van Wingerden
J.W.vanWingerden@TUDelft.nl

Michel Verhaegen
M.Verhaegen@TUDelft.nl

Delft Center for Systems and Control, Delft University of Technology, Delft, The Netherlands

Abstract

This paper is motivated by the closed-loop system identification problem of wind turbine systems. The data source for the system identification is based on controller-in-the-loop simulations of a typical multi-MW wind turbine. The paper shows the benefits of the Predictor-Based System IDentification (PBSID) method for closed-loop wind turbine model estimation. The PBSID identification technique does not require any controller related information, consequently the identified model becomes consistent no matter the wind turbine operates with or without controller in the loop. Being the wind turbine not asymptotically stable in open-loop, only closed-loop experiments are supported in the reality. This fact makes the PBSID method very attractive for the wind power community.

Keywords: wind turbines, subspace identification

1 Introduction

For the wind energy community, model-based controller design becomes more and more important. Model-based controller synthesis necessitates a nominal description of the real plant. Nominal description of the plant can either be derived from physical principles or using measured data, respectively. Therefore, the latter is considered as a preliminary phase on the way towards a controller design. System identification of wind turbines is not only important at the design of a new turbine setup, but also when existing devices has to be re-identified in order to create a more up-to-date and accurate model than the existing one. In this specific case, wind turbine system identification has to be performed in taking consideration the existing controller as well. Since, the paper focuses on the application of the PBSID method to the data provided by the TURBU simulator [1], the physical modeling concepts of the wind turbine are omitted. We use previously derived data to make off-line, more precisely batch-wise system identification.

Apart the application of the system identification methods, proper input signal selection and alternative (time and frequency domain) validation techniques are applied. To get an accurate model estimate, the information content of the input signal is analyzed. The excitation signal are designed conform with a real wind turbine identification scenario. Moreover, the paper suggests using regularization in order to overcome possible numerical problems, such as singularity of the regression problem. The identified models are analyzed both in time and frequency domain. Time domain analysis consist of the computation of the Variance-Accounted-For (VAF). Frequency domain validation of the identified models covers the comparative evaluation of the channel-wise frequency function.

2 Predictor-based subspace identification for LTI systems

In this section, the predictor-based subspace identification (PBSID) method for Linear Time-Invariant (LTI) systems operating in either open-loop or in closed-loop is presented.

2.1 Introduction to subspace methods

Subspace IDentification (SID) methods are efficient methods to identify state-space models from input and output measurements of a dynamic system, such as wind turbines. These methods store input and output data in structured block Hankel matrices, such that it is possible to retrieve certain subspaces that are related to the system matrices. They are candidates for the identification of wind turbine models due to several reasons. First, because SID methods can easily be extended from Single-Input and Single-Output (SISO) systems to Multiple-Input and Multiple-Output (MIMO) systems. Second, the key linear algebra steps, RQ, and SVD factorization, and the solution of a linear least-squares problem, give SID methods their efficiency, simplicity, and numerical stability.

In [2], a unified methodology is suggested in which many of the SID methods fall, such as Canonical Variate Analysis (CVA), N4SID [2], and MOESP [3] methods. However, it is known that these SID methods give biased results when the system to be modelled operates in closed-loop. The rationale behind it is that the future inputs are correlated with the past noises, due to the feedback controller. An alternative to the SID of SISO systems are the traditional Prediction Error Methods (PEM), see [4]. These methods uses a pre-defined parametrization of the model, for example an Auto Regressive with eXogenous inputs (ARX) model, where the parameters are obtained by minimizing a quadratic cost function. PEM can provide asymptotical consistent estimates in closed-loop if there is sufficient excitation from an external signal or a controller of sufficiently high order.

Recently a number of significant advances have been presented to identify LTI state-space models from measurements of dynamic systems operating in closed loop. These recent developments are extensively utilizing a Vector Auto Regressive with eXogenous inputs (VARX) model parametrized by markov parameters, which is in the case of SISO measurements similar to a high-order ARX model. The Predictor-Based Subspace IDentification (PBSID) [5] methods uses the estimated Markov parameters to constuct a Toeplitz matrix. Multiplication of the Toeplitz matrix with past input and output data, and applying a SVD, an estimation of the state sequence can be obtained. With the state sequence, it is straightforward to recover the system matrices. The advantage of the predictor-based approach over SID lies in the handling of the controller related information. The latter requires the controller related information (the structure such as the state space or at least a finite series of the step response functions).

2.2 Description of the used PBSID method

Consider that the dynamics of the system to be modelled can be written in the following minimal state-space model in the innovation form:

$$\begin{aligned} x_{k+1} &= Ax_k + Bu_k + Ke_k, \\ y_k &= Cx_k + Du_k + e_k, \end{aligned} \tag{1}$$

where $x_k \in \mathbb{R}^n$, $u_k \in \mathbb{R}^r$, $y_k \in \mathbb{R}^\ell$, are the predicted state and output vectors, and $e_k \in \mathbb{R}^\ell$ denotes the zero-mean white innovation process noise. The state-space matrices $A \in \mathbb{R}^{n\times n}$, $B \in \mathbb{R}^{n\times r}$, $C \in \mathbb{R}^{\ell\times n}$, $D \in \mathbb{R}^{\ell\times r}$, and $K \in \mathbb{R}^{n\times \ell}$ are also called the system, input, output, direct feedthrough, and Kalman gain matrices, respectively. We can rewrite (1) in predictor form as:

$$\begin{aligned} x_{k+1} &= \tilde{A}x_k + \tilde{B}u_k + Ky_k, \\ y_k &= Cx_k + Du_k + e_k, \end{aligned} \tag{2}$$

with $\tilde{A} = A - KC$, and $\tilde{B} = B - KD$. It is well-known that an state transformation does not change the input-output behaviour of a state-space system. With the above methodolgy we can only determine the system matrices up to a similarity transformation $T \in \mathbb{R}^{n\times n}$: $T^{-1}AT$, $T^{-1}B$, $T^{-1}K$, CT, and D. The identification problem can now be formulated as: Given the input sequence u_k, output sequence y_k over a time $k = \{0, \dots, N-1\}$; find all, if they exist, system matrices A, B, C, D, and K up to a global similarity transformation.

With assumptions that the system $\mathcal{S}$ to be modelled is considered observable and of fixed order, that the wind disturbance is zero-mean stationary and an ergodic white Gaussian noise sequence, that the input sequence u_k has sufficient excitation, that the feedback loop does not have direct feedthrough, the problem formulation does not require any other assumption on the correlation between the inputs and noise sequences, which opens the possibility to apply the algorithm in closed loop [6].

We define a past window denoted by $p \in \mathbb{N}^+$ and a future window denoted by $f \in \mathbb{N}^+$, where $n/\ell \leq f \leq p$. These windows are used to define the stacked vectors:

$$\bar{y}_{k-p,p} = \begin{bmatrix} y_{k-p} \\ y_{k-p+1} \\ \vdots \\ y_{k-1} \end{bmatrix}, \quad \bar{y}_{k,f} = \begin{bmatrix} y_k \\ y_{k+1} \\ \vdots \\ y_{k+f-1} \end{bmatrix},$$

Stacked vectors $\bar{u}_{k-p,p}$, $\bar{u}_{k,f}$, $\bar{e}_{k-p,p}$, and $\bar{e}_{k,f}$ are defined in a similar way. When a batch of N data is available, we can also define the stacked matrix Y:

$$Y = \begin{bmatrix} y_p, & \cdots, & y_{N-1} \end{bmatrix}.$$

The stacked vectors U, X are defined in a similar way. Further, we can define the stacked matrix $\bar{Y}_p$:

$$\bar{Y}_p = \begin{bmatrix} \bar{y}_{0,p}, & \cdots, & \bar{y}_{N-p,p} \end{bmatrix}.$$

Again, we can also obtain the stacked vectors $\bar{U}_p$.

We define the one-step-ahead VARX predictor as:

$$\hat{y}_{k|k-1,p} = \sum_{i=0}^{p} \tilde{\Xi}_i^{(u)} u_{k-i} + \sum_{i=1}^{p} \tilde{\Xi}_i^{(y)} y_{k-i}, \tag{3}$$

where $\hat{y}_{k|k-1,p}$ is the predicted output for time instant k using the given inputs of time instants $k, \dots, k-p$ and using the measured outputs of time instants $k-1, \dots, k-p$. Further, $\tilde{\Xi} \in \mathbb{R}^{\ell\times(p+1)(r+\ell)}$ is the set of Markov parameters to be estimated:

$$\tilde{\Xi} \triangleq \begin{bmatrix} \tilde{\Xi}_p^{(u)} & \dots & \tilde{\Xi}_0^{(u)} & \tilde{\Xi}_p^{(y)} & \dots & \tilde{\Xi}_1^{(y)} \end{bmatrix}.$$

In [6] it was shown that estimated VARX predictors, with large past window size, can provide asymptotical consistent estimated Markov parameters of the system to be modelled even with closed-loop data if there is sufficient excitation from an external signal or a controller of sufficiently high order to get an unique estimate. If the matrix $\Psi = \begin{bmatrix} \bar{U}^T & U^T & \bar{Y}^T \end{bmatrix}^T$ has full row rank, the Markov parameter set Ξ can be estimated by solving the following linear problem:

$$\min_{\Xi} \|Y - \Xi\Psi\|_F^2. \tag{4}$$

Now we introduce in this procedure an approximation for the state. The predicted state x_k is given by:

$$x_k = \tilde{A}^p x_{k-p} + \tilde{\mathcal{L}}\bar{u}_{k-p,p} + \tilde{\mathcal{K}}\bar{y}_{k-p,p}. \tag{5}$$

where $\mathcal{L}_k \in \mathbb{R}^{n\times pr}$ and $\mathcal{K}_k \in \mathbb{R}^{n\times pr}$ are the extended controllability matrices, and are given by:

$$\begin{aligned} \mathcal{L} &= \begin{bmatrix} \tilde{A}^{p-1}\tilde{B} & \cdots & \tilde{A}\tilde{B} & \tilde{B} \end{bmatrix}, \\ \mathcal{K} &= \begin{bmatrix} \tilde{A}^{p-1}K & \cdots & \tilde{A}K & K \end{bmatrix}. \end{aligned}$$

It can be shown that if the system in (2) is asymptotically stable, the contribution of the initial state x_{k-p} can be made arbitrarily small by making p large, see [6, 7]. The main assumption is that we assume the transition matrix is deadbeat with degree p, thus the matrix $\tilde{A}^j = 0$ for all $j \geq p$. With the assumption of nilpotency, the state x_k is now given by:

$$x_k = \tilde{\mathcal{L}}\bar{u}_{k-p,p} + \tilde{\mathcal{K}}\bar{y}_{k-p,p}. \tag{6}$$

In a number of closed-loop SID methods it is well known to make this approximation, see [5]. Observe that the product between the state and the observability matrix is given by:

$$\tilde{\Gamma}x_k = \widetilde{\Gamma\mathcal{L}}\bar{u}_{k-p,p} + \widetilde{\Gamma\mathcal{K}}\bar{y}_{k-p,p}, \tag{7}$$

where $\widetilde{\Gamma\mathcal{L}} \in \mathbb{R}^{f\ell \times pr}$ and $\widetilde{\Gamma\mathcal{K}} \in \mathbb{R}^{f\ell \times p\ell}$ are the products between the extended observability and the extended controllability matrices, and are given by:

$$\widetilde{\Gamma\mathcal{L}} = \begin{bmatrix} \tilde{\Xi}_p^{(u)} & \tilde{\Xi}_{p-1}^{(u)} & \cdots & \tilde{\Xi}_{p-2}^{(u)} & \cdots & \tilde{\Xi}_1^{(u)} \\ 0 & \tilde{\Xi}_p^{(u)} & \cdots & \tilde{\Xi}_{p-1}^{(u)} & \cdots & \tilde{\Xi}_2^{(u)} \\ \vdots & \ddots & \ddots & \vdots & \ddots & \vdots \\ 0 & \cdots & 0 & \tilde{\Xi}_p^{(u)} & \cdots & \tilde{\Xi}_f^{(u)} \end{bmatrix}, \tag{8}$$

$$\widetilde{\Gamma\mathcal{K}} = \begin{bmatrix} \tilde{\Xi}_p^{(y)} & \tilde{\Xi}_{p-1}^{(y)} & \cdots & \tilde{\Xi}_{p-2}^{(y)} & \cdots & \tilde{\Xi}_1^{(y)} \\ 0 & \tilde{\Xi}_p^{(y)} & \cdots & \tilde{\Xi}_{p-1}^{(y)} & \cdots & \tilde{\Xi}_2^{(y)} \\ \vdots & \ddots & \ddots & \vdots & \ddots & \vdots \\ 0 & \cdots & 0 & \tilde{\Xi}_p^{(y)} & \cdots & \tilde{\Xi}_f^{(y)} \end{bmatrix}. \tag{9}$$

These are upper block triangular matrices, because the introduced zeros come from the assumption of nilpotency. This implies that in the asymptotic case the approximation of the matrices $\widetilde{\Gamma\mathcal{L}}$ and $\widetilde{\Gamma\mathcal{K}}$ can be fully constructed by the Markov parameters $\tilde{\Xi}$.

After the construction of the matrices $\widetilde{\Gamma\mathcal{L}}$ and $\widetilde{\Gamma\mathcal{K}}$, we obtain the product between the observability matrix and the state sequence. The state vector can be estimated by solving an low-rank approximation problem given by:

$$\min_{\operatorname{rank}(\tilde{\Gamma}X)=n} \left\| Z - \tilde{\Gamma}X \right\|_F, \tag{10}$$

where $Z = \widetilde{\Gamma\mathcal{L}}\bar{U} + \widetilde{\Gamma\mathcal{K}}\bar{Y}$. The optimal low-rank approximant can be computed using the Singular Value Decomposition (SVD) as:

$$\widetilde{\Gamma\mathcal{L}}\bar{U} + \widetilde{\Gamma\mathcal{K}}\bar{Y} = \begin{bmatrix} U & U_\perp \end{bmatrix} \begin{bmatrix} \Sigma_n & 0 \\ 0 & \Sigma \end{bmatrix} \begin{bmatrix} V \\ V_\perp \end{bmatrix}, \tag{11}$$

The diagonal matrix Σ_n contains the n largest singular values, and the orthogonal matrices U and V contains the corresponding column and row space. Note that we can find the largest singular values by detecting a gap between the values. By truncation, i.e. by setting the $f\ell - n$ smallest singular values equal to zero, the obervability matrix and the state sequence are estimated as:

$$\hat{X} = \Sigma_n^{1/2} V. \tag{12}$$

When the state, input, and output sequence are known, the system matrices A, B, C, D, and K can be estimated by solving two linear problems obtained from (1).

2.3 On the selection of the windows

In the previous subsection, approximations are made which require the past window to be chosen as large as possible, so that the best VARX predictor is expected to be estimated. Thus, theoretically, the best linear model is estimated when the past window $p \to N$. However, in identification experiments it is most of the time needed to design the excitation signal such that it does not exceed the load specifications and ensures that the system to be identified operates around a particular operation point. In this case, especially with an low-order controller in the feedback loop, matrix Ψ becomes ill-conditioned for large past window sizes, because the input signals do not persistently excite the system enough. This means that matrix Ψ has nearly linear dependent rows, and is therefore very sensitive to pertubations on the measurement data. To avoid the ill-posed least squares problem a regularization quantity is included to the cost (4) and can be given by:

$$\min_{\Xi} \left[\|Y - \Xi\Psi\|_F^2 + \rho^2 \|\Xi\|_F^2 \right]. \tag{13}$$

A number of methods exist to determine ρ and solve the regularized least squares problem. In this paper, we have chosen to use the Tikhonov regularization method together with the Generalized Cross Validation (GCV) technique to determine the regularization value, because from experience this gives satisfactory results. In Figure 1, the trade off between the truncation error and condition number is illustrated for the TURBU simulation.

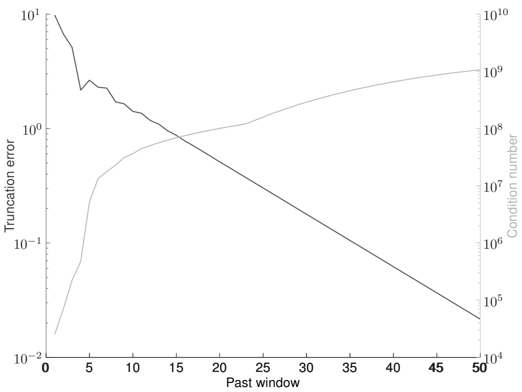

Figure 1: The truncation error of the VARX predictor and the condition number of Ψ with different values for the past window.

The selection of the future window f is even more difficult. It heavily depends on the input spectrum and system properties. It is suggested through simulation studies that a large future window is often better for identification experiments when the signal-to-noise ratio is low (averaging effect). Otherwise for higher signal-to-noise ratios, the optimal future window size has normally a smaller finite value.

3 Simulation Study

In this section we use a dynamic model of a wind turbine to demonstrate the effectiveness of the proposed algorithm. The TURBU simulator is used to generate input and output data sequence for closed-loop system identification. Due to the restrictions from the third party, most of the results in this chapter are normalized. This means that the frequencies, amplitudes, and other values illustrated in the figures are scaled to a common range of values.

3.1 Specifications of the TURBU model

We use an aero-elastic wind turbine model of a Horizontal-Axis Wind Turbine (HAWT) created with the ECN software TURBU [1] to demonstrate the closed-loop subspace LTI system identification algorithm. The model describes the rotational dynamics of a wind turbine around a particular operating point with wind speed $v = 18m/s$. The multi-body model contains around 100 states, representing the degrees of freedom in the foundation, tower, drive train, blades and the pitch servo actuators. The input signals to the model are three reference blade pitch angles θ_i and the reference generator torque T_{ge}. The outputs are defined as the generator speed Ω_{ge}, the tower top fore-aft velocity $\dot{x}_{nod}$ and tower top sideward's velocity $\dot{x}_{nay}$. The disturbance signals are the three blade effective wind signals v_i. The wind turbine system is not asymptotically stable, it contains an integrator. Therefore, a collective pitch controller and a generator torque controller are added in the feedback loop of the system for stabilization. Similar as in [8], the Coleman transformation have been used to transform the model to fixed-frame coordinates, such that it becomes LTI system. After the Coleman transformation, the system to be modelled fits in the linear model structure in (1). However, one is still interested in a low-dimensionality model for designing a controller.

3.2 Identification results of TURBU model

For consistent closed-loop model estimation of all frequencies, it is important that there would be sufficient excitation from an external excitation signal or a controller with sufficiently high order. The collective pitch controller, used to regulate the rotational speed, is based on a PI-compensator, and the torque controller has the form of a P-compensator. As the controllers are not sufficiently high order, we add additional excitation signal to the control signals. It is important to consider the effect of the excitation signal on the turbine loads. In [9], additional loads on the drive train and on the tower in fore-aft and sideward's direction are carefully inspected. From the load specifications of the wind turbine, the excitation signals for the collective pitch and generator torque inputs are created from a filtered PRBS. In Figure 2, the power spectral densities of both excitation signals are illustrated. It is clearly visible that filtering is applied at the higher frequencies (for a smoother signal) and also in the case of the collective pitch around the first natural frequency of the fore-aft displacement of the tower.

Not only, the dither signal at the plant input has different realizations, but also the wind disturbance (wind turbulence) v at the plant output. While identifying the system, two different wind disturbance realizations have been used; one for identification and one for validation (SWIFT generated at $v = 18$, von Karman type, with turbulence category A, [9]). We do not possess the wind gust model, we only use two alternative disturbance signals (for identification and validation respectively). Figure 3 depicts the frequency content of the wind realization applied. From the Figure, we can conclude the low pass nature of the normalized frequency content with the natural frequency around 0.8 [rad/sec].

Selection of the sample number N is of capital importance. The data length was chosen to be $N = 5000$ which corresponds to 33 min, the data is resampled to

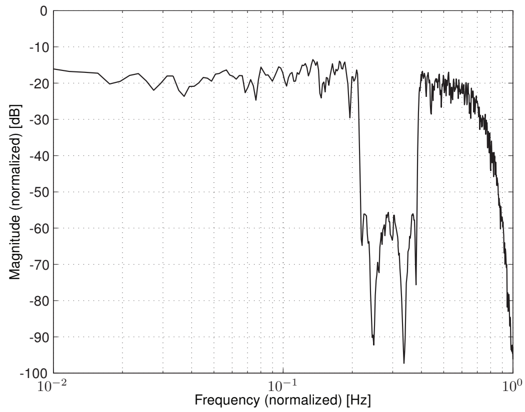

(a)

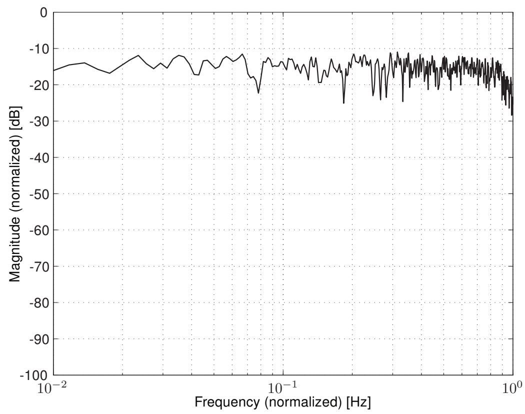

(b)

Figure 2: Spectral density diagrams of the additional excitation signals on the pitch (a) and the generator torque (b) inputs.

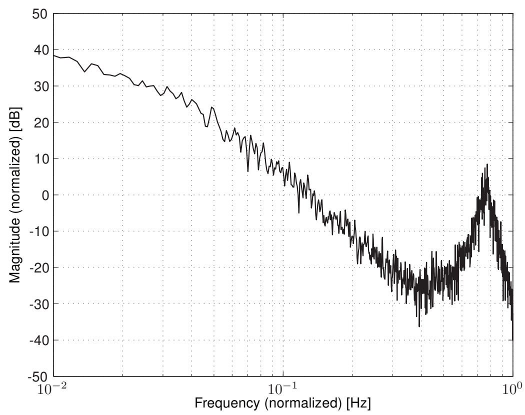

Figure 3: Spectral density diagram of the turbulence signals.

$h = 0.4$s. Longer data lengths give better results, however in reality the wind turbine stays only in an operation region for limited amount of time, depending on the wind. To investigate the sensitivity of the identification algorithm with respect to excitation, Monte-Carlo simulations with 100 runs are carried out. For each simulation a different realization of the filtered PRBS excitation signal is used.

The identified models are analyzed both in time and frequency domain. Time domain analysis consist of the computation of the Variance Accounted For (VAF). Frequency domain validation of the identified models covers the comparative evaluation of the channel-wise frequency function. The Variance-Accounted-For (VAF) percentage of the output variation that is explained by the model is defined as:

$$\mathrm{VAF} = \max\left\{1 - \frac{\mathrm{var}\left(Y - \hat{Y}\right)}{\mathrm{var}\left(Y\right)}, 0\right\} \times 100\%, \quad (14)$$

where *var* is an operator that computes the variance. The best FIT percentage of the output variation that is explained by the model is defined as:

$$\mathrm{FIT} = \max\left\{1 - \frac{\left\|\hat{Y} - Y\right\|_F^2}{\left\|Y - \mathrm{mean}\left(Y\right)\right\|_F^2}, 0\right\} \times 100\%, \quad (15)$$

where *mean* is an operator that computes the average.

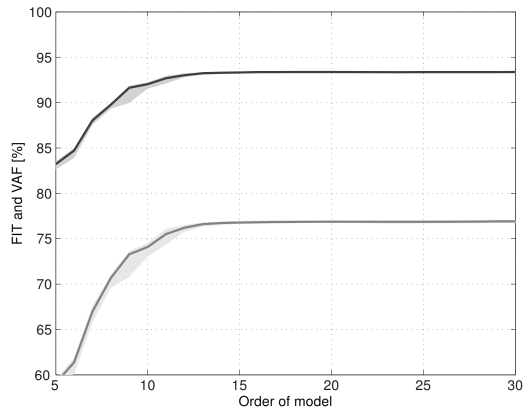

Figure 4: The mean FIT (grey) and VAF (black) against the order of the model identified with VARX-based PBSID. The grey region shows the errorbounds for the models of 100 Monte Carlo simulations. ($p = 50$, $f = 15$)

One of the most difficult challenge while using identification methods is certainly the selection of the appropriate model order, the state dimension n. Theoretically, the model behind the TURBU simulator has almost 100 states. First, not all of the states are relevant. Second, for the possible control synthesis low-order models are preferred and then with the help of robust control methodology the neglected dynamical part can also be taken into consideration. Figure 4 shows the VAF and the FIT values of the identified and then validated models versus the selected model order. One can see the difference between the identification for low order models (under 15) and the high order above 15 where not only the average VAF/FIT values are lower for low model order, but also the error bounds are larger around. Maximal VAF/FIT values are $93\%/77\%$ after $n \geq 15$.

We have to investigate the influence of the window size p, f which are indespensable for PBSID. Up to this moment we assumed $p = 50$ and $f = 15$. Theoretically the only constraint on the window sizes is to consider $p \geq f$. Figure 5 gives details on the window size selection. Information in Figure5 shows the nature of the VARX model structure, which provides more accurate mean VAF value when the window size goes large. Based on the above experiments, large past horizon is crucial and the future horizon can be relatively small. These facts motivate the choice of the following identification windows for linear TURBU model identification. When using regularization, the VAF results become structured reflecting the effect of the truncation error (high in case of low past window size). We can see slightly higher average VAF value when no regularization is applied. We choose $p = 50$ and $f = 15$ with regularization.

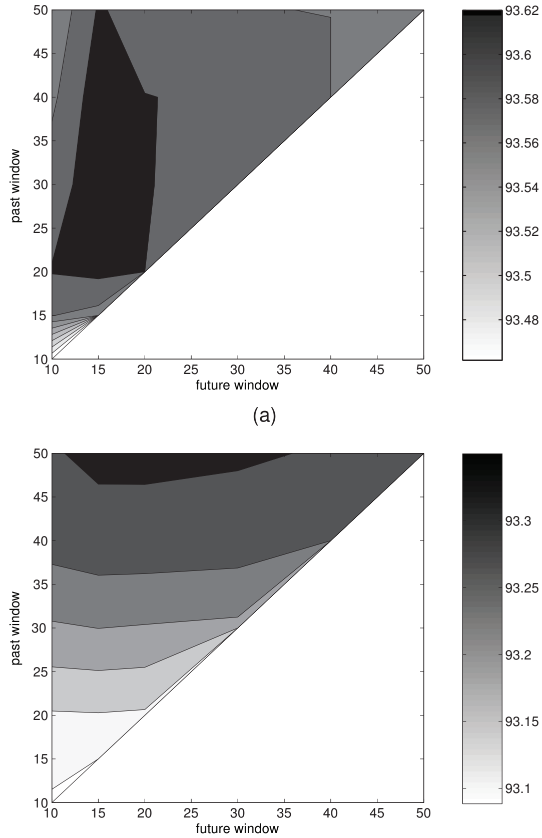

(b)

Figure 5: The mean VAF against the past window and future window of the model identified, where (a) is without and (b) is with regularization. ($n = 16$)

The most relevant transfer functions are the following: the one from the collective pitch angle $\theta_{col} \rightarrow \Omega_{ge}, \dot{x}_{nod}$, and the transfer from the generator torque $T_{ge} \rightarrow \Omega_{ge}, \dot{x}_{nay}$. Using the afford-mentioned identification technique, four relevant input-output transfer functions are validated. Figure 6 shows the comparative analysis of the frequency functions based on the pre-selected model order and identification window sizes. Note that

MIMO system identification is performed and Bode magnitude diagrams are plotted respectively. As a generic conclusion, one can see accurate identification of the TURBU model around the natural frequencies (at the high frequency part of the examined frequency range). The transfers from the pitch angle are more consistent to the TURBU model than those from the generator torque.

4 Conclusion

The paper concentrated on the use of an identification technique over wind turbine model identification for controller design, and showed the benefits of the application of the predictor-based subspace identification method for linear time invariant systems operating in closed loop.

5 Acknowledgements

This research is supported under the WE@SEA program of SenterNovem, an agency of the Dutch Ministry of Economic Affairs to promote sustainable development and innovation. The authors like to thank Stoyan Kanev of ECN, who provided the TURBU data.

References

[1] T. van Engelen. Control design based on aero-hydro-servo-elastic linear models from TURBU (ECN). In *Proceedings of the European Wind Energy Conference (EWEC)*, Milan, Italy, 2007.

[2] P. Van Overschee and B. De Moor. *Subspace Identification for Linear Systems; Theory, Implementation, Applications*. Kluwer Academic Publishers, 1996.

[3] M. Verhaegen and V. Verdult. *Filtering and System Identification*. Cambridge University Press, 2007.

[4] L. Ljung. *System Identification: Theory for the user, 2nd Edition*. Prentice Hall, 1999.

[5] A. Chiuso. The role of vector auto regressive modeling in predictor based subspace identification. *Automatica*, 43(6):1034–1048, 2007.

[6] A. Chiuso and G. Picci. Consistency analysis of some closed-loop subspace identification methods. *Automatica*, 41(3):377–391, 2005.

[7] A. Chiuso. Asymptotic variance of closed-loop subspace identification methods. *IEEE Transactions on Automatic Control*, 51(8):1299–1341, 2006.

[8] T. G. van Engelen, H. Markou, T. Buhl, and B. Marrant. Morphological study of aeroelastic control concepts for wind turbines. Technical report, Energy research Centre of the Netherlands, July 2007.

[9] S. Kanev. System identification for wind turbine applications: WE@SEA project 2007-014, phase 1. Technical report, Energy research Centre of the Netherlands, 2008.

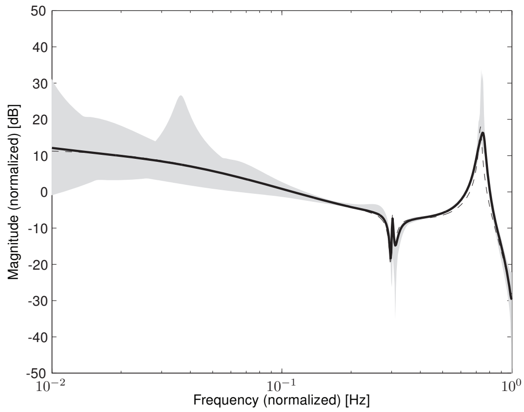

(a) From θ_{col} to Ω_{ge}

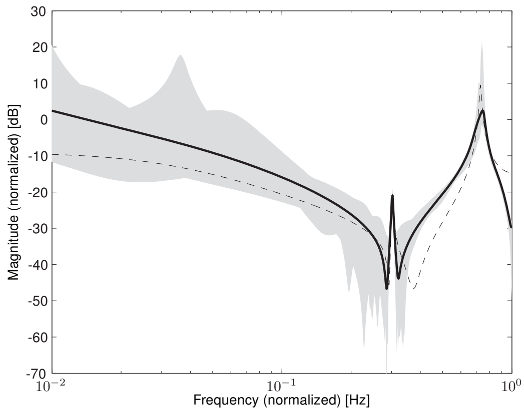

(b) From T_{ge} to Ω_{ge}

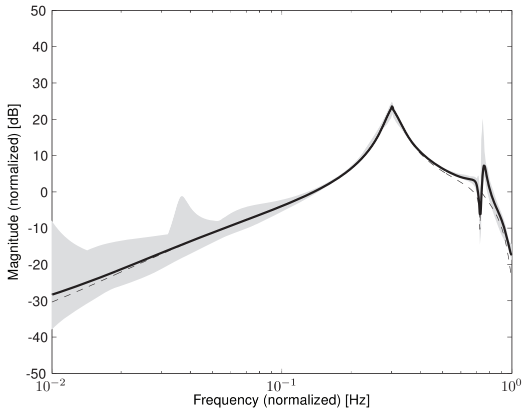

(c) From θ_{col} to $\dot{x}_{nod}$

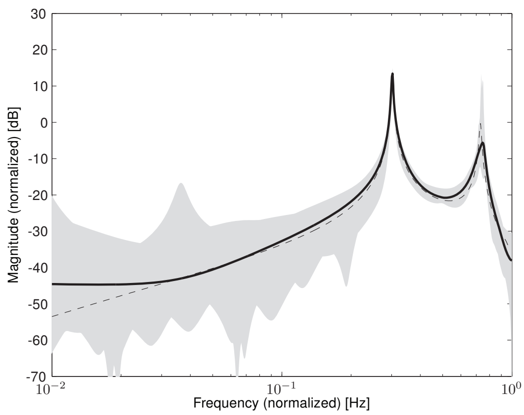

(d) From T_{ge} to $\dot{x}_{nay}$

Figure 6: Bode diagrams of the TURBU model (dashed) and the identified model with the highest VAF value (bold). The other 99 models are within the grey region. $(n = 16, p = 50, f = 15)$